Printed UWB Antenna Operating Over Multiple Mobile Wireless Standards

Leonardo Lizzi, *Student Member, IEEE*, Renzo Azaro, *Member, IEEE*, Giacomo Oliveri, *Member, IEEE*, and Andrea Massa, *Member, IEEE*

***Abstract*—In this letter, a spline-shaped ultrawideband (UWB) antenna enabling simultaneous operability over multiple mobile wireless standards—namely the DCS, PCS, UMTS, and ISM bands—is proposed. The antenna is expected to exhibit a good impedance matching and stable radiation features within the whole range of working frequencies. A set of numerical and experimental results is reported to assess the efficiency of the proposed design.**

***Index Terms*—Antenna synthesis, mobile wireless standards, spline curves, ultrawideband (UWB) antennas.**

I. Introduction

In THE last few years, new and different mobile standards have been defined under the growing demand for wireless services characterized by high-data-rate transmissions and increased mobility. Accordingly, modern communication devices are expected to effectively operate over different frequency bands as the DCS (1.71–1.88 GHz), the PCS (1.85–1.99 GHz), the UMTS (1.92–2.17 GHz), and the ISM (2.40–2.485 GHz) bands.

In this framework, the design of the radiating systems is a key issue to be carefully addressed for realizing devices with reliable multiple-standard operation capability. Toward this end, antennas are usually required to exhibit not only good impedance matching, but also stable radiation properties. This problem has been widely dealt with within the scientific community, and different solutions have been proposed over the years. Many strategies rely on the use of the printed circuit board (PCB) technology because of the several advantages such as low profile, light weight, robustness, cheap cost, and suitability for mass production [1].

As for multiband antennas, standard solutions are generally based on suitable modifications of a reference geometry. Starting from a planar inverted-F antenna (PIFA), two different models of dual-band antennas have been obtained in [2] by adding a spiral geometry and modifying the feed structure, respectively. Elsewhere [3], a dual-band behavior has been yielded by adding a properly shaped stub to the ground plane of a simple monopole radiator. Differently, two bent slots have been used in [4] to provide a pentagonal antenna with good dual stopband rejection characteristics and a three-band capability. An alternative solution is reported in [5], where a broadband spiral antenna is transformed into a dual-band antenna by integrating a frequency selective surface (FSS) as ground plane.

On the other hand, fractal-shaped antennas have recently proved to be very promising for synthesizing miniaturized multiband antennas thanks to their self-similarity properties. Representative examples can be found in [6]–[12]. However, despite suitable impedance matching, fractal radiators do not usually show stable radiation properties within wide operating bands. As a matter of fact, the distributions of the surface currents turn out to be different than generating different patterns of radiation. Therefore, wideband or ultrawideband (UWB) antennas are generally exploited to yield a uniform behavior when the bands of interest are close to each other or even slightly overlapped (e.g., the DCS and PCS bands).

Several shapes and structures have been proposed over the years to synthesize UWB radiators. In [13], the UWB behavior has been obtained by sequentially inserting three notches in the two corners of a rectangular patch connected to a feed line, while circular contours have been proposed for UWB applications in [14] and [15]. By generalizing the use of curvilinear geometries, an approach for the synthesis of UWB printed monopoles based on a spline representation of the antenna has been first proposed in [16] and successively exploited in [17] and [18] for synthesizing miniaturized elements.

In this letter, a printed UWB antenna able to effectively support multiple mobile wireless standards is presented. The antenna synthesis is carried out by considering a spline-based representation of the radiator and applying an efficient particle swarm optimization (PSO) [19] procedure to obtain a good impedance matching and stable radiation properties over the frequency range of interest. The synthesized antenna has been built and tested. Both numerical and experimental evaluations have been performed to assess the effectiveness as well as the reliability of the proposed solution.

The outline of the letter is as follows. The antenna geometry is described in Section II. Section III provides a numerical/experimental analysis on the performances of the synthesized antenna, while some concluding remarks are reported in Section IV.

II. Antenna Design

The design procedure is aimed at obtaining an antenna enabling operability within the DCS, PCS, UMTS, and ISM bands. Toward this end, the antenna is required to exhibit a good impedance matching and stable radiation properties in the frequency range from $f_{\mathrm{L}} = 1.7$ GHz up to $f_{\mathrm{H}} = 2.5$ GHz.

Manuscript received October 16, 2011; revised November 21, 2011; accepted December 05, 2011. Date of publication December 14, 2011; date of current version December 26, 2011.

The authors are with the University of Trento, Trento 38050, Italy (e-mail: andrea.massa@ing.unitn.it).

Color versions of one or more of the figures in this letter are available online at http://ieeexplore.ieee.org.

Digital Object Identifier 10.1109/LAWP.2011.2179631

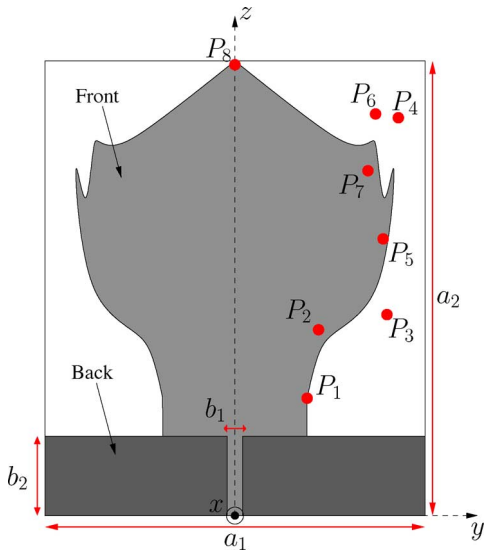

Fig. 1. Antenna geometry.

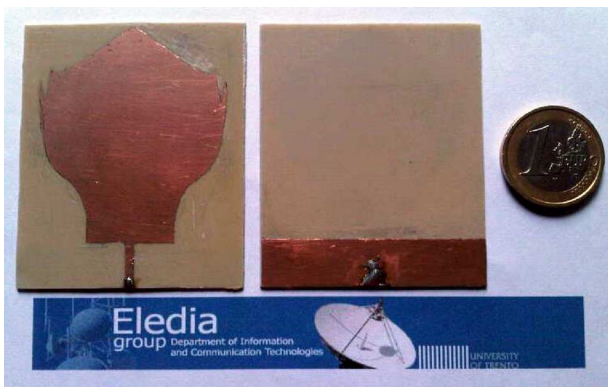

Fig. 2. Antenna prototype.

TABLE I
ANTENNA GEOMETRICAL DESCRIPTORS

Antenna Descriptors [mm]			
Geometrical Parameters			
a_1	a_2	b_1	b_2
51.2	60.0	1.8	10.5
Spline Control Points			
P_1	P_2	P_3	P_4
(9.5, 15.0)	(11.0, 24.5)	(20.0, 26.5)	(21.5, 52.5)
P_5	P_6	P_7	P_8
(19.5, 36.5)	(18.5, 53.0)	(17.5, 45.5)	(0.0, 60.0)

The first requirement has been conveniently set in terms of scattering parameters by imposing the following constraint:

$$|S_{11}(f)| \leq -10 \text{ dB} \qquad f \in \{f_{\text{L}}, f_{\text{H}}\}. \tag{1}$$

As for the radiation behavior, the following condition has been forced on the the antenna total gain G_{tot} to ensure an almost omnidirectional radiation along the horizontal plane ($\theta = 90°$). More specifically

$$\Delta G_{\text{tot}}(\theta, \varphi) \leq 5 \text{ dB} \qquad \forall \theta = 90°, \varphi \in \{0°, 360°\} \tag{2}$$

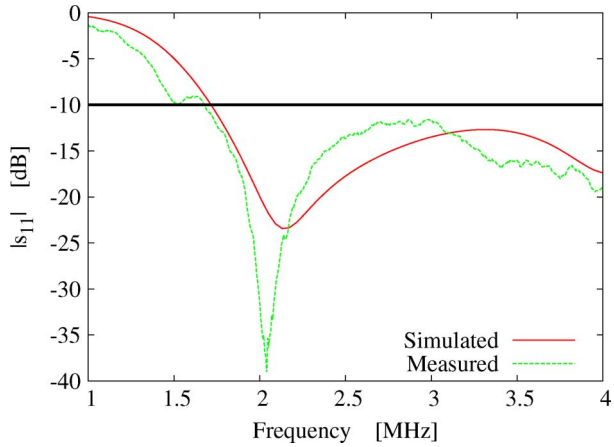

Fig. 3. Simulated and measured values of the magnitude of S_{11}.

TABLE II
ELECTRICAL PERFORMANCES

	Operating Band ($\lvert s_{11}\rvert \leq -10\,dB$)
Simulated	$1.70 - 4.00\,GHz$
Measured	$1.67 - 4.00\,GHz$

with

$$\Delta G_{\text{tot}}(\theta, \varphi) = \max_f G_{\text{tot}}(f, \theta, \varphi) + - \min_f G_{\text{tot}}(f, \theta, \varphi) \; f \in \{f_{\text{L}}, f_{\text{H}}\} \tag{3}$$

being the maximum gain variation in the whole band of interest along the direction (θ, φ).

To fulfill these requirements, the PSO-based automatic synthesis procedure proposed in [16] has been applied. Such an approach consists of the following key points [16]: 1) the UWB antenna shape representation, which exploits a combination of parametric descriptors and spline curves (Fig. 1); 2) the UWB antenna system characterization, done through a suitable method of moments (MoM)-based solver (because of the frequency-domain formulation of the requirements); 3) the identification of the final antenna shape, carried out through a PSO-based strategy [19] aimed at optimizing the antenna descriptors. More specifically, the PSO explores the solution space through a swarm of R randomly initialized "particles" that are iteratively updated according to the associated *functional* values, computed taking into account (1) and (2) [16]. The optimization procedure ends when a maximum number of iteration K is reached, or when the functional value is smaller than a user-defined convergence threshold η [16]. For the design at hand, the following parameter setup has been considered [19]: $R = 8, \eta = 10^{-5}$, and $K = 200$. As a result, the geometry in Fig. 1 characterized by the geometrical parameters in Table I has been determined. The antenna structure is composed by two metallic layers printed on both sides of a dielectric substrate, whose horizontal and vertical extensions are denoted by a_1 and a_2, respectively. On the front side, the metallic shape is symmetric along the z-axis, and it includes a feed line of dimension $b_1 \times b_2$ as well as a radiating patch. The patch contour has been modeled with a

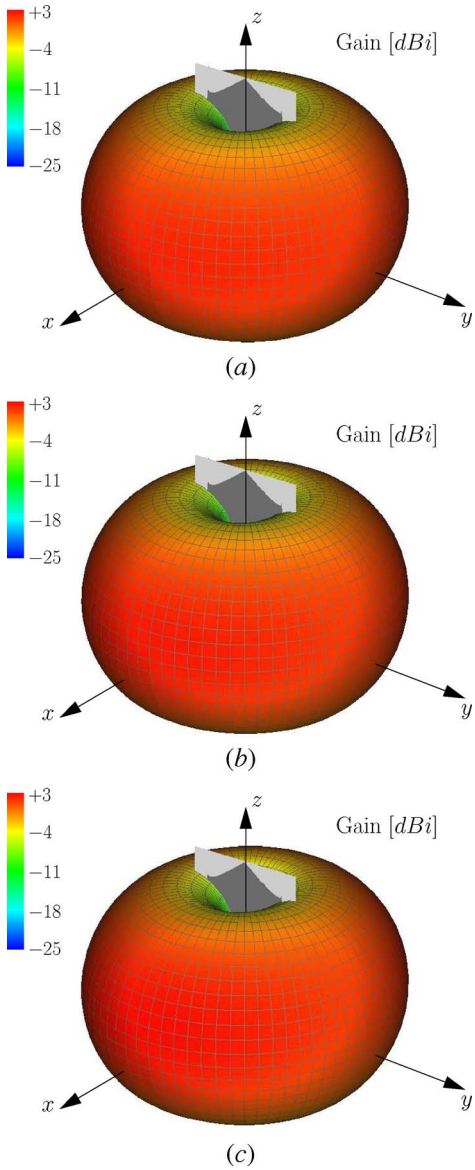

Fig. 4. Three-dimensional radiation patterns at (a) $f_{\rm L} = 1.7$ GHz, (b) $f_{\rm R1} = 2.1$ GHz, and (c) $f_{\rm H} = 2.5$ GHz.

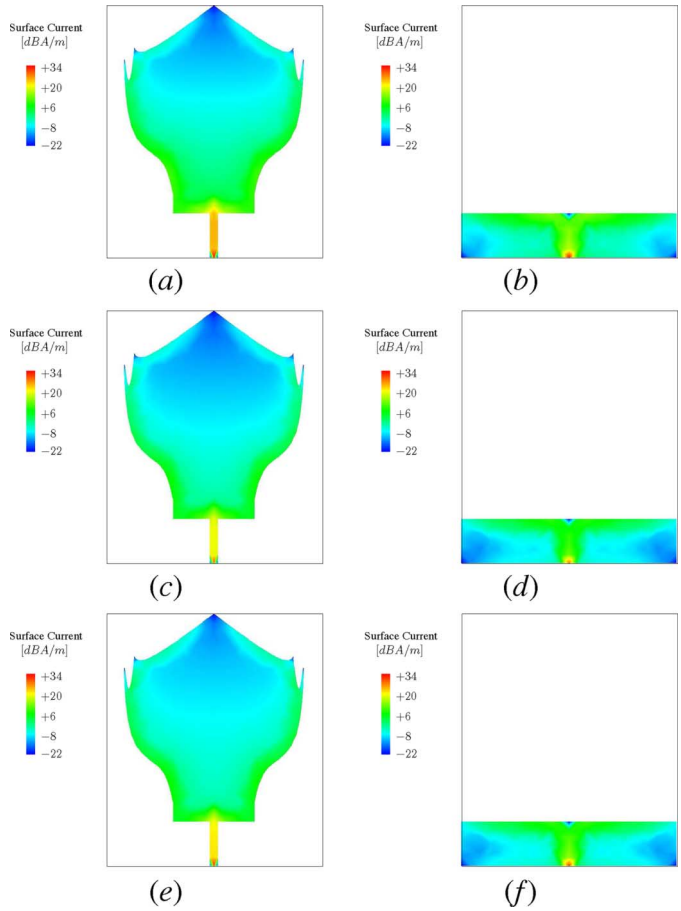

Fig. 5. Surface current on (a), (c), (e) the front and (b), (d), (f) the back of the antenna at (a), (b) $f_{\rm L} = 1.7$ GHz, (c), (d) $f_{\rm R1} = 2.1$ GHz, and (e), (f) $f_{\rm H} = 2.5$ GHz.

spline curve univocally defined by the $N = 8$ control points $P_n = (y_n, z_n), n = 1, \ldots, N$ in Table I. On the backside, the ground plane occupies the dark region indicated in Fig. 1.

III. Numerical and Experimental Validation

To assess the effectiveness of the synthesized antenna, both numerical and experimental tests have been carried out, and the results are briefly summarized in this section. Toward this end, a prototype of the antenna has been realized on an Arlon dielectric substrate (Arlon 25N with thickness 0.76 mm) characterized by $\epsilon_{\rm r} = 3.38$ and $\tan\delta = 0.0025$ (Fig. 2).

As far as the electrical performances are concerned, an indication on the impedance matching over the extended frequency range from 1 up to 4 GHz is given in Fig. 3. The antenna fulfills the project requirements since the magnitude values of S_{11} turn out to be smaller than -10 dB in the range 1.70–4.00 GHz (Table II) with a resonance at $f_{\rm R1} = 2.1$ GHz. Moreover, the experimental data are in good agreement with the simulated results besides some differences due to the fabrication imperfections in the realization of the prototype.

Concerning the radiation properties of the prototype, the antenna presents almost invariant radiation properties as confirmed by the three-dimensional plots of the simulated antenna total gain in Fig. 4. More in detail, the radiation properties of the synthesized radiator have been evaluated at the two extremes of the band of interest (i.e., $f_{\rm L} = 1.7$ GHz and $f_{\rm H} = 2.5$ GHz) as well as at the intermediate frequency value, $f_{\rm R1} = 2.1$ GHz. As it can be observed, the antenna behaves like a monopole with an almost unaltered radiation pattern over the whole frequency band. This is further confirmed by the similar plots of the surface current distributions in Fig. 5. The currents flow from the antenna feeding point to the top of the radiating patch along the same path whatever the considered frequency [Fig. 5(a), (c), and (e)]. As expected, they concentrate in the feed line because of its small dimension and at the edges of the patch with amplitude values decreasing along the path. Such a behavior is not surprising since the vertical extension of the patch is equal to $0.35\lambda_{\rm R1}, \lambda_{\rm R1}$, with the wavelength being at $f_{\rm R1} = 2.1$ GHz, and the radiating structure turns out to be slightly longer than a $\lambda/4$ structure with a surface current distribution close to that of a standard quarter-wave monopole.

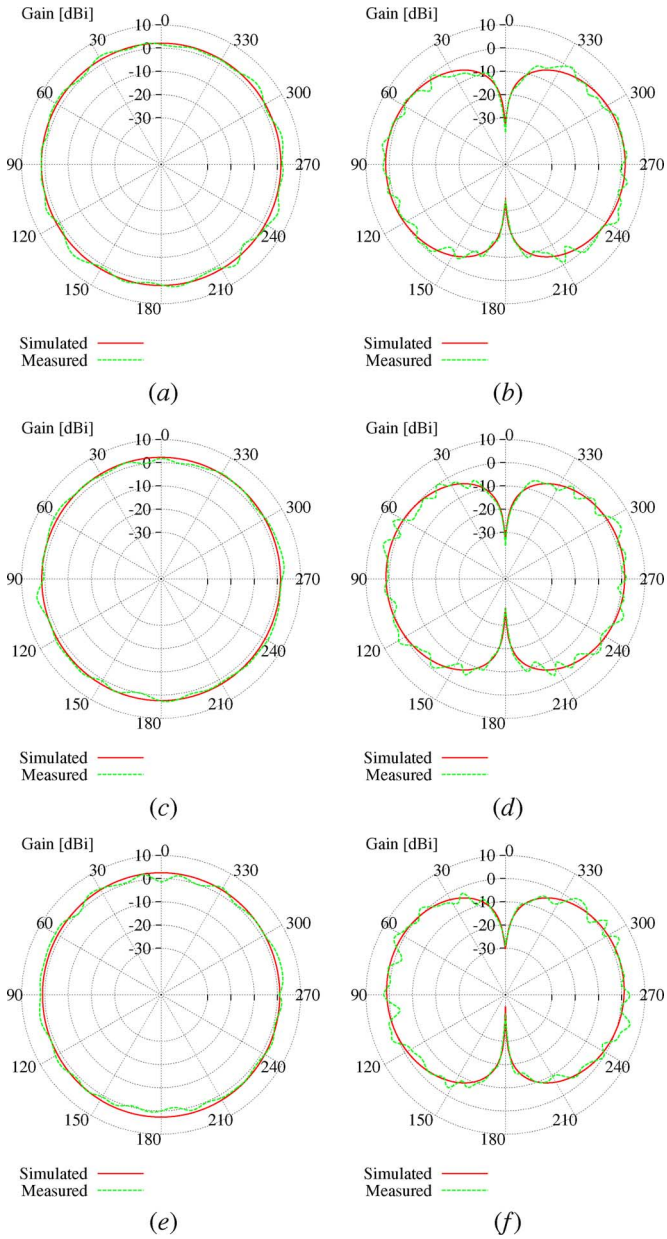

Fig. 6. Simulated and measured radiation patterns. Cut planes at (a), (c), (e) $\theta = 90°$ and (b), (d), (f) at $\phi = 90°$ when (a), (b) $f_{\rm L} = 1.7$ GHz, (c), (d) $f_{\rm R1} = 2.1$ GHz, and (e), (f) $f_{\rm H} = 2.5$ GHz.

On the back [Fig. 5(b), (d), and (f)], the current mainly flows at the center of the ground plane due to the presence of the feed line on the opposite side of the substrate and toward the top edge of the metallic region.

To assess and confirm the outcomes from the simulated results on the radiation properties of the prototype, the total gain has been measured at the two cut planes $\theta = 90°$ and $\varphi = 90°$ (Fig. 6). As expected, the measurements satisfactorily match the simulated data with a variation lower than 3 dB in the horizontal plane [Fig. 6(a), (c), and (e)].

IV. Conclusion

In this letter, a spline-shaped UWB antenna able to support multiple mobile wireless standards has been proposed. The antenna has been synthesized to guarantee a suitable impedance matching as well as stable radiation properties over the frequency range 1.7–2.5 GHz, where the DCS, PCS, UMTS, and ISM services are located. The efficiency of the antenna design and of the corresponding prototype have been assessed through numerical simulations and experimental measurements.

References

[1] L. Lizzi, F. Viani, and A. Massa, "Dual-band spline-shaped PCB antenna for Wi-Fi applications," *IEEE Antennas Wireless Propag. Lett.*, vol. 8, pp. 616–619, 2009.

[2] Y.-S. Wang, M.-C. Lee, and S.-J. Chung, "Two PIFA-related miniaturized dual-band antennas," *IEEE Trans. Antennas Propag.*, vol. 55, no. 3, pp. 805–811, Mar. 2007.

[3] W. Hu, Y. Z. Yin, X. Yang, and X. S. Ren, "Compact printed antenna with h-shaped stub for dual-band operation," *Electron. Lett.*, vol. 46, no. 25, pp. 1644–1645, 2010.

[4] H. W. Liu, C. H. Ku, and C. F. Yang, "Novel CPW-fed planar monopole antenna for WiMAX/WLAN applications," *IEEE Antennas Wireless Propag. Lett.*, vol. 9, pp. 240–243, 2010.

[5] C. N. Chiu and W. H. Chuang, "A novel dual-band spiral antenna for a satellite and terrestrial communication system," *IEEE Antennas Wireless Propag. Lett.*, vol. 8, pp. 624–626, 2009.

[6] J. Pourahmadazar, C. Ghobadi, J. Nourinia, and H. Shirzad, "Multiband ring fractal monopole antenna for mobile devices," *IEEE Antennas Wireless Propag. Lett.*, vol. 9, pp. 863–866, 2010.

[7] R. Azaro, E. Zeni, P. Rocca, and A. Massa, "Synthesis of a Galileo and Wi-Max three-band fractal-eroded patch antenna," *IEEE Antennas Wireless Propag. Lett.*, vol. 6, pp. 510–514, 2007.

[8] E. Zeni, R. Azaro, P. Rocca, and A. Massa, "A quad-band patch antenna for Galileo and Wi-Max services," *Electron. Lett.*, vol. 43, no. 18, pp. 960–962, 2007.

[9] R. Azaro, F. Viani, L. Lizzi, E. Zeni, and A. Massa, "A monopolar quadband antenna based on a Hilbert self-affine pre-fractal geometry," *IEEE Antennas Wireless Propag. Lett.*, vol. 8, pp. 177–180, 2008.

[10] R. Azaro, E. Zeni, P. Rocca, and A. Massa, "Innovative design of a planar fractal-shaped GPS/GSM/Wi-Fi antenna," *Microw. Opt. Technol. Lett.*, vol. 50, no. 3, pp. 825–829, 2008.

[11] L. Lizzi, F. Viani, E. Zeni, and A. Massa, "A DVBH/GSM/UMTS planar antenna for multimode wireless devices," *IEEE Antennas Wireless Propag. Lett.*, vol. 8, pp. 568–571, 2009.

[12] L. Lizzi and G. Oliveri, "Hybrid design of a fractal-shaped GSM/UMTS antenna," *J. Electromagn. Waves Appl.*, vol. 24, no. 5/6, pp. 707–719, 2010.

[13] R. Zaker and A. Abdipour, "A very compact ultrawideband printed omnidirectional monopole antenna," *IEEE Antennas Wireless Propag. Lett.*, vol. 9, pp. 471–473, 2010.

[14] J. Liang, C. C. Chiau, X. Chen, and C. G. Parini, "Study of a printed circular disc monopole antenna for UWB systems," *IEEE Trans. Antennas Propag.*, vol. 53, no. 11, pp. 3500–3504, Nov. 2005.

[15] O. Ahmed and A. R. Sebak, "A printed monopole antenna with two steps and a circular slot for UWB applications," *IEEE Antennas Wireless Propag. Lett.*, vol. 7, pp. 411–413, 2008.

[16] L. Lizzi, F. Viani, R. Azaro, and A. Massa, "A PSO-driven spline-based shaping approach for ultrawideband (UWB) antenna synthesis," *IEEE Trans. Antennas Propag.*, vol. 56, no. 8, pp. 2613–2621, Aug. 2008.

[17] F. Viani, L. Lizzi, R. Azaro, and A. Massa, "A miniaturized UWB antenna for wireless dongle devices," *IEEE Antennas Wireless Propag. Lett.*, vol. 7, pp. 714–717, 2008.

[18] L. Lizzi, F. Viani, R. Azaro, and A. Massa, "Design of a miniaturized planar antenna for FCC-UWB communication systems," *Microw. Opt. Technol. Lett.*, vol. 50, no. 7, pp. 1975–1978, 2008.

[19] J. Robinson and Y. Rahmat-Samii, "Particle swarm optimization in electromagnetics," *IEEE Trans. Antennas Propag.*, vol. 52, no. 2, pp. 397–407, Feb. 2004.